

Article

Using Electric Field to Improve the Effect of Microbial-Induced Carbonate Precipitation

Jinxiang Deng ^{1,2}, Mengjie Li ^{1,2}, Yakun Tian ^{1,2}, Zhijun Zhang ^{1,2,*}, Lingling Wu ^{1,2,*} and Lin Hu ^{1,2}

¹ School of Resource & Environment and Safety Engineering, University of South China, Hengyang 421001, China

² Hunan Province & Hengyang City Engineering Technology Research Center for Disaster Prediction and Control on Mining Geotechnical Engineering, Hengyang 421001, China

* Correspondence: 130000148665@usc.edu.cn (Z.Z.); 2013000541@usc.edu.cn (L.W.)

Abstract: The precipitation of calcium carbonate induced by *Sporosarcina pasteurii* (*S. pasteurii*) has garnered considerable attention as a novel rock and soil reinforcement technique. The content and structure of calcium carbonate produced through this reaction play a crucial role in determining the rocks' and soil's reinforcement effects in the later stages. Different potential gradients were introduced during the bacterial culture process to enhance the performance of the cementation and mineralization reactions of the bacterial solution to investigate the effects of electrification on the physical and chemical characteristics, such as the growth and reproduction of *S. pasteurii*. The results demonstrate that the concentration, activity, and number of viable bacteria of *S. pasteurii* were substantially enhanced under an electric field, particularly the weak electric field generated by 0.5 V/cm. The increased number of bacteria provides more nucleation sites for calcium carbonate deposition. Moreover, as the urease activity increased, the calcium carbonate content generated under an electric potential gradient of 0.5 V/cm surpassed that of other potential gradient groups. The growth rate increased by 9.78% compared to the calcium carbonate induced without electrification. Significantly, the suitable electric field enhances the crystal morphology of calcium carbonate and augments its quantity, thereby offering a novel approach for utilizing MICP in enhancing soil strength, controlling water pollution, and mitigating seepage. These findings elevate the applicability of microbial mineralization in engineering practices.

Keywords: microbial biomineralization; *Sporosarcina pasteurii*; potential gradient; calcium carbonate



Citation: Deng, J.; Li, M.; Tian, Y.; Zhang, Z.; Wu, L.; Hu, L. Using Electric Field to Improve the Effect of Microbial-Induced Carbonate Precipitation. *Sustainability* **2023**, *15*, 5901. <https://doi.org/10.3390/su15075901>

Academic Editors: Hong-Wei Yang, Shuren Wang and Chen Cao

Received: 21 February 2023

Revised: 25 March 2023

Accepted: 27 March 2023

Published: 28 March 2023



Copyright: © 2023 by the authors. Licensee MDPI, Basel, Switzerland. This article is an open access article distributed under the terms and conditions of the Creative Commons Attribution (CC BY) license (<https://creativecommons.org/licenses/by/4.0/>).

1. Introduction

The swift advancement of technology and the economy has resulted in the excessive depletion of the Earth's resources. In new construction projects, cement and other cementitious materials are essential [1,2]. However, the production and utilization of cement can readily lead to environmental contamination. In recent years, microbial cement, a novel reinforcement methodology, has captured the attention of countless researchers due to its inherent benefits of environmental conservation, convenience, and pollution-free attributes, aligned with the objective of eco-friendly and green development. Feng et al. [3] investigated a new variety of bacterial-based self-repairing concrete using microbial-induced calcium carbonate precipitation. They fabricated self-healing concrete beam samples incorporating bacteria as a mending agent and polyvinyl alcohol fibers. The outcomes indicated that the flexural strength of beams could be improved by roughly 14%. Sj et al. [4] synthesized the research progress of enhancing the longevity of industrial-by-product-modified concrete and provided insights for the future incorporation of microbial treatment into concrete. Yu et al. [5] utilized microorganisms to hydrolyze organophosphate monoesters to yield phosphate nanomaterials, which exhibited greater stability in structures. The gelation performance of phosphate precipitation induced by microorganisms was exceptional.

Additionally, this technique demonstrated potential applications in removing heavy metals, treating solid waste, and consolidating sandy soil. Zheng and Qian [6] utilized microbial-induced calcification (MICP) technology to prevent cracks in cement-based materials. The outcomes revealed that this technology could increase the area repair rate to 96% and the corresponding waterproof repair resistance to 85%, effectively improving the self-healing efficacy of cracks in later stages of cement-based materials.

Microbial cementation comprises a succession of biochemical reactions that utilize microorganisms to instigate the precipitation of calcium carbonate (MICP) and leverage the precipitated calcite to ameliorate the mechanical characteristics of the rock and soil that necessitate reinforcement. Almajed et al. [7] presented a summary of the applicability, advantages, and disadvantages of MICP in soil treatment and elucidated the mechanism of MICP in both natural and laboratory environments. To realize on-site implementation, they proposed a site-specific method to execute on-site. Feng et al. [8] elaborated on the research findings of MICP technology on recycled aggregate reinforcement and listed the factors influencing the reinforcement effect of recycled aggregate. Post-MICP treatment, the aggregate properties were improved. Gao and Dai [9] suggested optimizing the medium to enhance the cementing effect. Optimizing the medium increased calcium carbonate precipitation at the contact point, enhanced the cementing effect, and increased strength by 1.2–4 times. Lin et al. [10] utilized numerical simulation to determine the dominant calcium carbonate distribution in the pore space and discussed the influence of calcium carbonate distribution on small strain stiffness and permeability. The results indicated that the numerical model could estimate the permeability after MICP treatment. Zhang et al. [11] conducted an experimental comparison of MICP tailings reinforcement technology affected by the seepage field and unaffected by the seepage field. It was discovered that under the influence of the seepage field, the total pores were comparatively reduced, the shear strength was lowered, and the distribution of calcium carbonate was more irregular. This suggests that seepage is one of the primary reasons for the instability of the tailings dam.

MICP is a multi-faceted process with numerous factors that exert influence, including the concentration of reinforcement bacteria, their activity [7,12], the cultural environment in which they grow, the duration and temperature of the culture, and the pH level [13–15]. Presently, the efficacy of MICP is restricted to specific practical applications. To enhance the reinforcement performance and rate, a few researchers have scrutinized calcium carbonate production by varying different culture conditions [16–18]. Among these, Okwadha and Li [19] examined the impact of bacterial species, cementing solution concentration, bacterial concentration, and reaction temperature on calcium carbonate deposition and ascertained that the maximum deposit of calcium carbonate occurs when the concentration of calcium ions is 0.25 mol/L, the concentration of urea is 0.666 mol/L, the bacterial concentration is 2.3×10^8 cells/mL. Several other scholars have evaluated the efficiency of the strengthening bacteria in hydrolyzing urea [20], which facilitates a more uniform strengthening effect. Research has revealed that the alkaline environment yields a higher calcium carbonate content and a better cementing effect than other pH culture conditions. In order to enhance the effectiveness of microbial reinforcement, the primary objective is to elevate the amount of calcium carbonate generated and enhance the crystal composition of calcium carbonate. Numerous studies have demonstrated that the crystal form of calcium carbonate will develop different crystal morphologies in the course of MICP, owing to different reactants [21]; Wei et al. [22] observed five distinct crystal morphologies of calcium carbonate grown in the MICP process via scanning electron microscope (SEM), namely cube, diamond, polyhedral layer, sphere, and irregular shape. By modulating the biological activity of microorganisms, researchers can manipulate calcium carbonate's crystallization rate and alter the resulting crystals' morphology [23]. As a result, promoting the biological activity of reinforcing bacteria can lead to an increase in the quantity of precipitated calcium carbonate precipitation, and improving the effect of microbial reinforcement [24] are effective means of accomplishing the goal.

The promotion of microbial activity can be achieved by implementing an electric field. Since the surface of microbial cells typically carries a charge, applying a potential can prompt microorganisms to undergo biochemical reactions within a specific action dimension created by the generated electric field. Research conducted by some scholars [25,26] has demonstrated that voltage can provide a certain degree of electric oxidation intensity, effectively stimulating microbial growth, enhancing microbial degradation activity, and enabling them to play a more effective role in soil remediation. In soil pollution control, the process of electric field migration can significantly improve the uniform distribution of microorganisms. Mena et al. [27] utilized a direct current in microbial remediation of soil hydrocarbons, applying an electric potential gradient (0–2 V/cm) to the culture of diesel degradation microorganisms, which increased the degradation rate. It was also found that a particular electric field had no significant negative impact on microbial activity. Cheng et al. [28] discovered that the electrokinetic (EK) phenomenon could enhance the mobility and redistribution of mineralized bacteria in heterogeneous rock and soil, thereby significantly promoting bioaugmentation. Weak potential gradients (1 V/cm) enable bacteria to evolve from a loose to a tightly bound state.

Moreover, the electric field promotes bacterial adhesion, fluid contact between anions and cations, organic carbon, and bacteria to stimulate bacterial proliferation. The results also reveal that the electric field is more effective in stimulating bacterial proliferation than transporting bacteria. Few studies have been conducted on applying electric fields in microbial induced mineralization. Therefore, based on the beneficial effect of the electric field on bacteria, the role of an electric field in MICP mineralization reaction was further explored by stimulating the proliferation of mineralized microorganisms and creating more induced precipitation nucleation sites.

This study assesses the viability of utilizing electric fields to enhance microbial-induced mineralization. By examining the effect of different electric fields on the MICP reaction, critical parameters such as the intensity and duration of each potential gradient and the impact of electric field regulation on precipitated calcium carbonate yield were analyzed for their energy efficiency range. Furthermore, to explore the impact of electric fields on microbial-induced mineralization of calcium carbonate, scanning electron microscopy (SEM), Fourier transform infrared spectroscopy (FT-IR), and X-ray diffraction (XRD) were employed.

2. Materials and Methods

2.1. Test Bacteria

The microorganisms used in the experiment (*Sporosarcina pasteurii*, see Figure 1) were purchased from the National Culture Collection and Management Center (No.: ATCC11859). *S. pasteurii* is an anaerobic bacteria [29], rod-shaped, with a bacterial length of 2 to 3 μm and good environmental tolerance. It is a moderately alkaliphilic bacteria growing at 15 to 37 $^{\circ}\text{C}$. The composition of the liquid medium is 15 g/L of casein (CAS: 91079-40-2), 5 g/L of soya peptone (CAS: 91079-46-8), 5 g/L of sodium chloride, and 20 g/L of urea. The required volume of deionized water was added to the liquid medium, the pH was adjusted to 7.3 [18], the bottle was divided into a 250 mL conical flask, and was finally sterilize in a high-temperature pot at 121 $^{\circ}\text{C}$ for 20 min (urea in the culture medium is filtered and sterilized to remove miscellaneous bacteria) for later use. The solid medium was added with 20 g of agar powder based on the liquid medium. After sterilization in the same step, the solution was poured into a Petri dish to make a flat plate for later use.

2.2. Equipment and Materials

The experiment was divided into two main parts. In the first part, physical and chemical parameters such as bacterial concentration and activity under standard culture conditions were determined by cultivating *S. pasteurii*. The optimal stage for introducing an electric field was identified. In the second part, the effect of the electric field on the mineralization reaction induced by *S. pasteurii* was investigated by introducing an electric field into the cultivated *S. pasteurii*. The flow diagram of the test is shown in Figure 2.

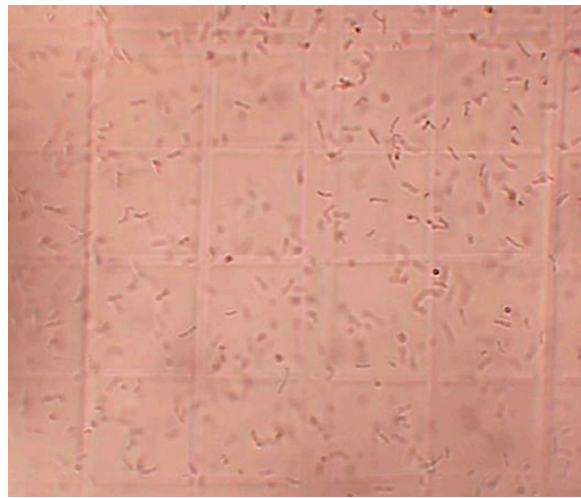


Figure 1. Morphological characteristics of *S. pasteurii*.

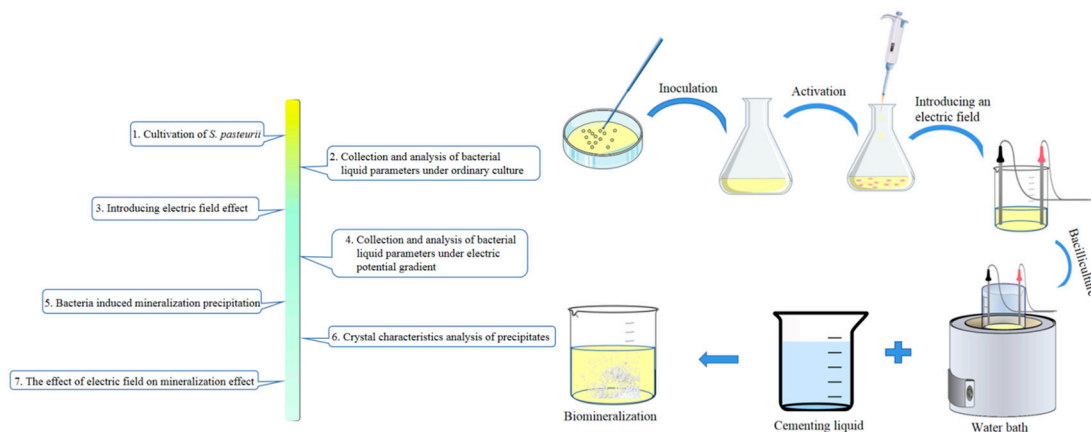


Figure 2. Schematic diagram of test flow.

The main instruments and equipment in the early bacterial culture process include a biochemical incubator (model: LRH-250F), aseptic operation table (model: SW-CJ-1FD), high-temperature sterilization pot (model: GI-54DWS), pH meter (model: PHSJ-3G), conductivity meter (model: TTS-11A), constant temperature oscillation box (model: ZQZY-78AV), protein-nucleic acid analyzer (model: BioPotometer), etc. The leading equipment in the subsequent energization includes a DC power supply (model: MS1002D), graphite electrode, culture tank (self-made microbial constant temperature culture system, See Section 3.2 for details), a peristaltic pump (model: BT100-2J), magnetic stirrer (model: CJJ79-1), and thermometer (Hengyang, China).

2.3. Experiment Method

The steps of this method are as follows. Determine the optical density at 600 nm (OD_{600}) [30] value of the activated and expanded *S. pasteurii* solution with a blank medium using a protein-nucleic acid analyzer and adjust it to 1.0 ± 0.05 . Next, inoculate 1.0 mL of the bacterial solution into 100 mL of medium in an Erlenmeyer flask and place it in a constant temperature shaking box at 30°C with 150 r/min. The bacterial solution is sampled every 2 h for 18 times over 36 h (all measurements were performed at least in triplicate, and the data were plotted with Origin and analyzed statistically); three repeatability measurements were taken and recorded when the samples were tested. The corresponding growth curve is determined and plotted. The concentration of bacteria is expressed by the value of OD_{600} measured by the turbidimetric method [30,31]. As the bacteria grow, the medium solution

gradually becomes turbid. The bacterial concentration is proportional to the absorbance, which is why the OD value is measured. Researchers commonly use formula (1) to convert specific bacterial counts [30,32].

$$Y = 8.59 \times 10^7 \times Z^{1.3627} \quad (1)$$

Here, Z represents the value of the measured OD₆₀₀, and Y represents the number of bacteria (cells/mL).

The above equation applies only when the OD₆₀₀ is within 0.2 to 0.8. If the bacterial concentration exceeds the upper limit of the measurement range, the resulting count will include both viable and nonviable cells. Hence, the spreading plate method was employed to accurately determine bacterial growth during cultivation by determining viable cell counts. Additionally, the pH of the bacterial solution was directly measured using a pH meter.

To investigate the impact of electric fields on *S. pasteurii* mineralization, four applied potential gradients of 0.5 V/cm, 0.75 V/cm, 1.0 V/cm, and 1.25 V/cm were established. The bacteria liquid with the most optimal bacterial activity period was selected in the preliminary test and subjected to electric current. After the power was switched on, measurements were taken every 10 min, and plates were coated every 30 min, with 18 samples collected. Each gradient was subjected to electric current for 3 h. After the application of electric fields, the bacterial solution was introduced to the cementing solution to initiate the mineralization process, following which the extent of calcium carbonate precipitation was quantified.

3. Results and Discussion

3.1. Cultivation of *S. pasteurii*

3.1.1. Bacterial Growth

Figure 3 shows the growth curve of the tested *S. pasteurii* after 36 h of continuous culture. Bacterial growth generally consists of four stages: lag phase, log phase, stable phase, and decay phase. In this experiment, the lag phase is not apparent because the bacteria have been repeatedly cultivated by the research group and thoroughly adapted to the culture environment. As shown in the figure, the bacteria increase faster and become relatively stable after reaching a maximum concentration at around 24 h. During the initial stage of the culture, the pH of the bacterial solution quickly rose from its initial value of 7.3 and attained a value of 9.0 after about 4 h.

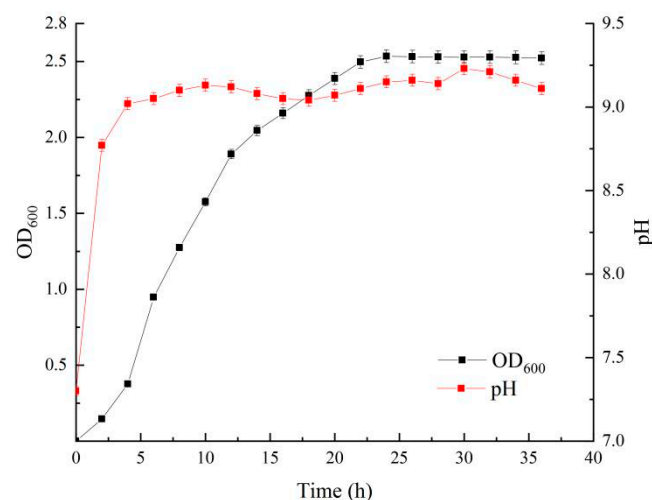


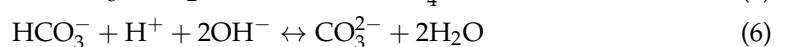
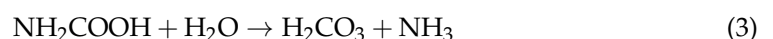
Figure 3. Growth curve of *S. pasteurii* and change trend of pH value.

Due to its alkalophilic nature, the growth rate of *S. pasteurii* is relatively slow in the neutral environment at the beginning of its growth cycle. As the bacteria grow, metabolic

activities result in the production of urease. Urea in the culture medium freely diffuses into bacterial cells and is converted into a nitrogen source by urease. Specifically, urease catalyzes the hydrolysis of urea to generate ammonium and carbonate ions following a series of chemical reactions. Firstly, urea is hydrolyzed into Carbamate and ammonia through the action of urease (as depicted in Formula (2)). When exposed to water, Carbamate readily decomposes into carbonic acid and ammonia (as shown in Formula (3)). Subsequently, carbonic acid and ammonia undergo hydrolysis in an equilibrium reaction to produce bicarbonate, carbonate, ammonium, and hydroxide ions (as depicted in Formulas (4) to (6)). As a result of the action of urease, the nitrogen source required for bacterial proliferation is rapidly obtained, allowing the bacteria to enter the logarithmic phase.

Upon the hydrolysis of urea, the subsequent release of ammonium and carbonate ions into the environment engendered a rise in pH levels, creating an alkaline habitat that favored bacterial growth. Upon examination of Figure 3, it can be observed that the proliferation of bacteria exhibited a slow pace during the nascent stages of growth. The pH levels experienced a rapid escalation during this phase, suggesting that the bacteria primarily enhanced the pH levels of their surroundings via the hydrolysis of urea during the initial stages, thus creating an environment for subsequent, expeditious growth. The growth curve of bacteria and the alteration of pH levels of bacterial solution underwent a definite time lag, which could be attributed to the delayed effect of the interplay between the pH levels and bacterial growth, which depends on how *S. pasteurii* obtains energy. Research conducted by Cuzman et al. [33] revealed that the synthesis of ATP and the transportation of *S. pasteurii* are inextricably linked to the production of ammonium ions within the bacteria. The findings indicated that the most appropriate pH level for the normal culture of *S. pasteurii* is roughly 9.25, whereas the intracellular pH value of bacteria hovers around 8.4. Upon the diffusion of urea into the bacteria, the ammonium ions, produced by the hydrolysis of urease, are gradually released into the extracellular space [34]. The bacteria display an accelerated growth rate when the pH levels in vivo and extracellular space differ. However, when the environmental pH exceeds 9.0, the pace of bacterial growth slackens. This is due to the concentration ratio of ammonium ion to ammonia molecule being 70:30 within the bacterial cell, at pH 8.4. The variance in ammonium concentration between the interior and exterior of the cell prompts the ammonium radical to diffuse out of the cell.

On the one hand, the diffusion of ammonium radicals contributes to the alkalinity of the environment, thereby promoting bacterial growth. On the other hand, a portion of the ammonium radicals converts into ammonia molecules and protons. The proton concentration gradient generated by the bacteria is higher than inside the cell, creating an effective proton kinetic potential. Consequently, the cell membrane's proton pump (ATP synthase) is activated to synthesize ATP [33]. This series of energy conversions effectively facilitates proliferation and increases the pH value of the bacterial solution. Due to the time sequence of the biochemical reactions, there is a certain delay between the growth curve of bacteria and the pH value change in the bacterial solution, which underscores the close relationship between bacterial growth and pH value changes.



3.1.2. Viability and Bacterial Count

S. pasteurii can induce precipitation of calcium carbonate and initiate mineralization reactions, as it secretes urease enzymes with highly efficient hydrolysis capabilities. The level of urease activity and the timing of the addition of the cementing liquid determines the

amount of calcium carbonate produced. Whiffin et al. [35] discovered in 2007 that the urease activity of the bacterial solution can be determined by measuring the change in conductivity of the solution. During the hydrolysis of urea by urease, the ion concentration in the bacterial solution rapidly increases, leading to a corresponding increase in conductivity value. The research findings demonstrate a positive correlation between the urease activity of the bacterial liquid and the rate of conductivity change, which can be mathematically represented using conversion Formulas (7) and (8).

$$U = 11.11f \quad (7)$$

$$S = U/OD_{600} \quad (8)$$

In the formula, U is the urease activity of the bacterial liquid (ms/cm/min); f is the rate of change in conductivity (ms/min); S is the unit urease activity (ms/cm/min).

Add 3 mL of the tested bacterial solution to 27 mL of 1.5 mol/L urea and use a conductivity meter to measure the change in conductivity of the mixed solution within 5 min after thorough mixing. The urease activity of the bacterial liquid and its change in unit urease activity can be obtained by conversion, as depicted in Figure 4. This study's lag period is not apparent due to the prior cultivation of *S. pasteurii* in multiple cycles. It can be observed from the figure that the bacterial adaptation to the culture environment is faster in the 0–2 h timeframe, and the bacterial count increases gradually. Between 2 and 16 h, the bacteria begin to grow after an adaptation period. The bacterial cell division leads to a linear increase in the bacterial concentration in the culture medium. This stage corresponds to the logarithmic phase of bacterial culture, during which the growth rate is maximized.

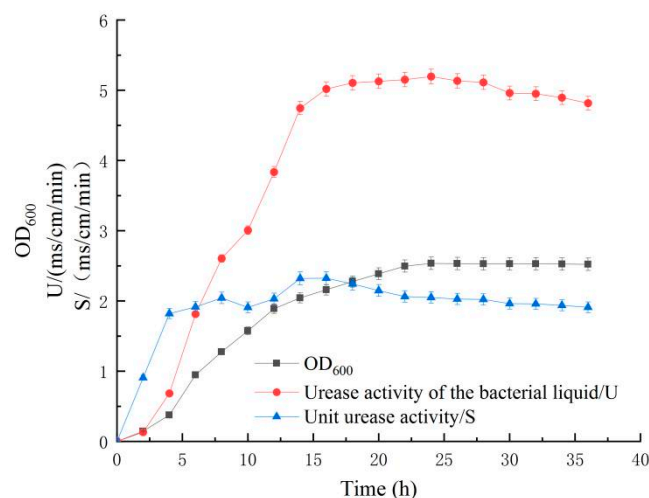


Figure 4. Changes in urease activity during bacterial growth.

After 16 h, stability is achieved as the concentration of bacterial solution reaches its maximum value. The nutrient substances in the culture medium are increasingly consumed, and the toxic products produced by bacterial metabolism lead to a decline in the metabolic capacity of the bacterial cells due to accumulation, causing a decrease in the rate of bacterial proliferation. Over time, the number of newly proliferated and dying bacteria tends to balance gradually. Later, with the influence of unfavourable factors, the decay rate becomes gradually greater than the new ones, causing the bacterial solution concentration to decrease. The trend of the urease activity in the bacterial solution displayed in the figure is strongly correlated with the changes in the concentration of the bacterial solution. As time elapses, the urease activity of the bacterial solution progressively increases along with the bacterial concentration. During this period, the capacity of the bacteria to hydrolyze urea continually intensifies, ultimately resulting in maximal urease activity after approximately 24 h. Additionally, the unit urease activity of the bacterial solution is influenced by its

concentration, and its fluctuation is notable, gradually decreasing subsequent to reaching its peak value at 16 h. Notably, the urease activity of the bacterial solution is critical in bacterial mineralization.

In order to investigate alterations in colony-forming units (CFU) of viable bacteria in *S. pasteurii* under standard culture conditions, samples were collected from 10 to 28 h post-culture initiation and cultured using the plate colony counting method. The resultant alteration trend in the viable bacterial count is presented in Figure 5 ($p < 0.05$). Sampling time nodes in the figure comprised logarithmic, late stable periods, and others. It can be observed from the figure that the viable bacterial count increased linearly with the logarithmic phase's growth in the bacterial concentration. The highest viable bacteria count was observed around 14 h, reaching 3.395×10^8 cells/mL. Subsequently, due to unfavourable factors such as bacterial liquid metabolism in the culture environment, the overall bacterial concentration reduced, leading to a decline in viable bacterial proportion and a continuous reduction in the viable bacterial count. The considerable changes in the number of viable bacteria substantially affect the unit urease activity in the bacterial solution.

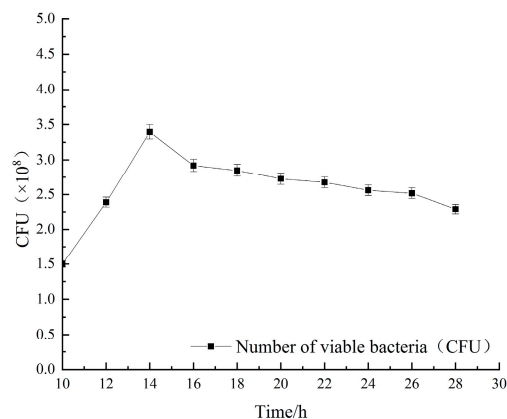


Figure 5. Changes in the number of viable bacteria of *S. pasteurii*.

3.2. The Effect of External Electric Field on Bacteria

To examine the impact of an external electric field on the growth and cementation process of *S. pasteurii*, a custom-made microbial constant temperature culture system was employed for experimentation (Figure 6). Since the optimal cultivation temperature for *S. pasteurii* is approximately 30 °C, a constant temperature water bath with a circulating water pump was employed, with real-time temperature regulation by a thermometer to maintain the culture tank's ambient temperature at 30 °C. A magnetic stirrer was situated beneath the bath heating tank, and the bacterial liquid was stirred by driving previously placed magnetic beads in the culture tank. The potential gradient of the applied electric field was managed at 0.5–1.25 V/cm (voltage ranging from 7.5 V to 18.75 V). During the initial bacterial liquid culture phase, the bacterial liquid (24 h) was analyzed when the concentration reached its maximum, and electrified culture was initiated. The energization duration was set at 3 h, and the sampling frequency was set at 10 min per time. In order to determine changes in the bacterial count during energization, a coating plate test was conducted every 30 min. Two tanks were employed in the experiment, one for energized bacterial culture and the other for bacterial-induced calcium carbonate precipitation under energization.

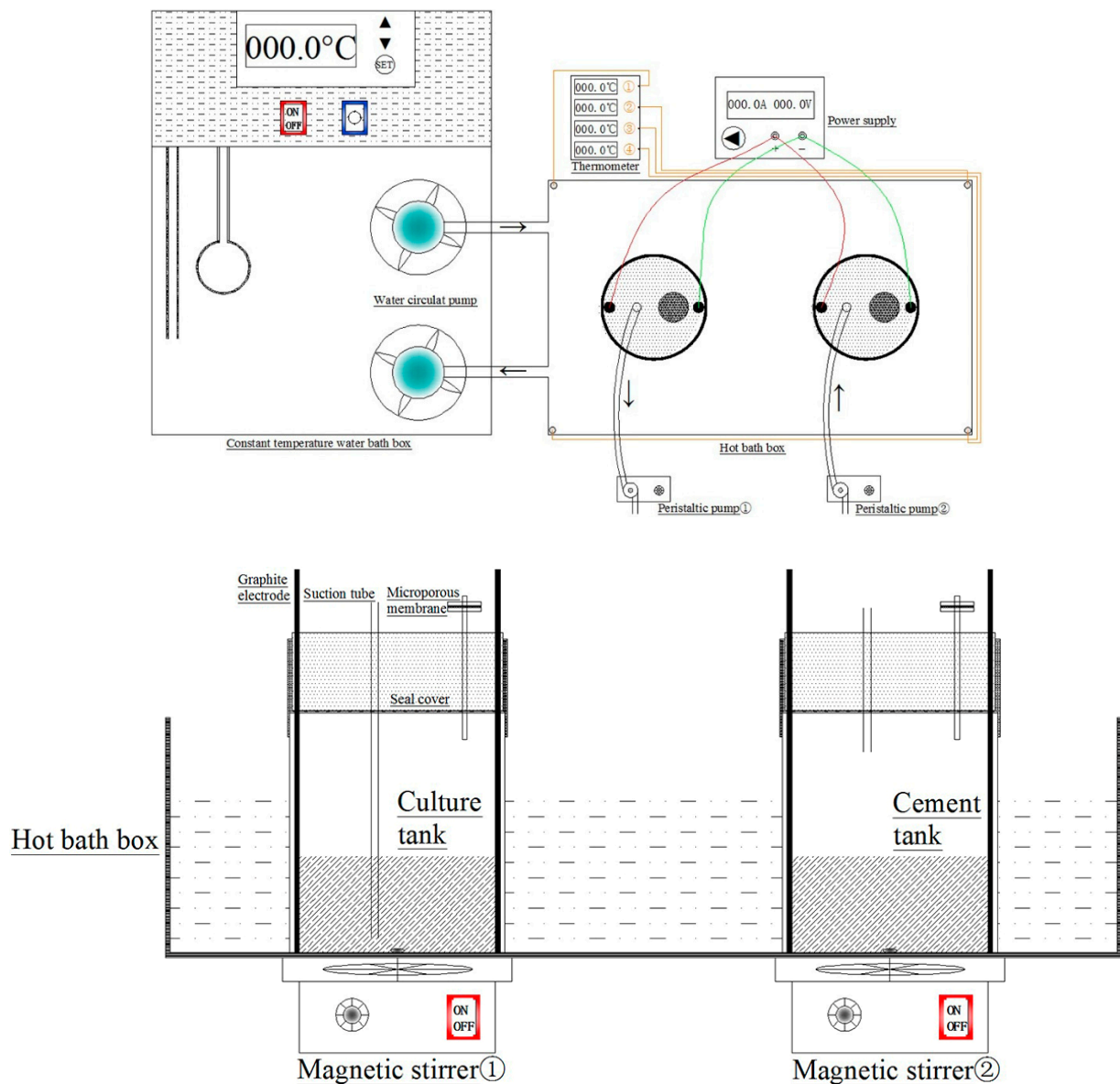


Figure 6. Test devise.

3.2.1. Bacteria Growing in the Electric Field

The growth curve of *S. pasteurii* under different potential gradients is illustrated in Figure 7. The effects of various potential gradients on the bacteria display notable

differences. As a result of bacteria's distinct sensitivity to electric fields, the overall growth trend is characterized by an initial increase followed by a decrease. After applying power, electrolysis and bubbles emerge at the contact between the electrode and the bacterial liquid in the culture tank. At the electrode, oxygen evolution occurs at the anode (Equation (9)), and hydrogen evolution takes place at the cathode (Equation (10)).

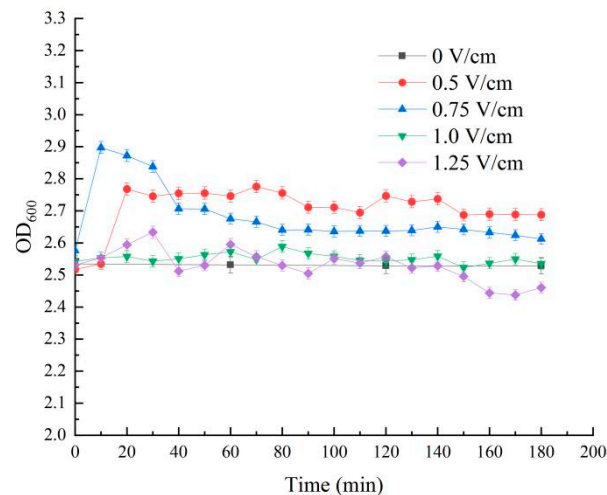
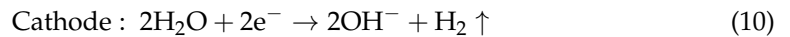
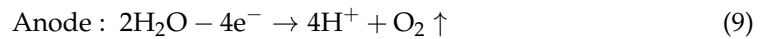


Figure 7. The growth curve of *S. pasteurii* in different potential gradients.

In the initial phase of electrification, the hydrogen and oxygen generated through electrolysis via an external electric field exhibit a specific stimulus on the growth and proliferation of bacteria. Nonetheless, with the amplification of the gradient, the tolerance threshold of the bacteria surpasses. Consequently, the development of bacteria becomes inhibited under the influence of the electric field. The figure displays the usage of the 0 V/cm group as a control group and 1 V/cm gradient as the boundary, the growth curve of bacteria increased obviously under the weak potential gradient, and the concentration increased significantly at the initial stage. However, with the elongation of the energization time, the optical density (OD) value under the 0.75 V/cm gradient begins to decrease. As *S. pasteurii* is an anaerobic bacterium, the oxygen produced at the anode expedites the growth of bacteria.

Nevertheless, with the continued effect of the electric field, the bacterial cells become incapable of tolerating the abnormally high electric potential, leading to changes in the permeability of the cell membrane. The cell membrane is chiefly made up of a double-layered phospholipid molecular arrangement. When an electric field acts on the cell membrane, ionization is accelerated, causing alterations in the osmotic pressure within and outside the membrane, ultimately resulting in bacterial cell rupture and death and thus decreasing the concentration of the bacterial solution. Upon the potential gradient's elevation, the OD value shift range gradually declines. The vehement electrolysis reaction at the electrode and the "inactivation" caused by the direct contact between the bacteria and the electrode are among the reasons for bacterial death. The excessive electric potential exerts an inhibitory impact on bacterial growth. When a gradient of 1.0 V/cm is applied, the growth curve of bacteria is akin to that of the control group. However, it appears unaffected by the electric field from the changing trend. As the gradient rises to 1.25 V/cm, the concentration of bacteria fluctuates significantly, the overall trend being downward, thus impeding bacterial growth. A comparison of the results of the five experimental groups reveals that a potential gradient of 0.5 V/cm is the most suitable gradient for maximizing

the growth-promoting effect on *S. pasteurii*. The concentration of the bacterial solution is maximally increased, thus signifying the most suitable potential gradient.

Moreover, in the realm of bacterial response to electric fields, Sun et al. [36] conducted electrophoresis experiments on *Escherichia coli* and discovered that the bacteria attained the maximal living amount under an electric field of 0.0455 mA/cm. Compared to bacteria cultured under normal conditions, the OD value of the bacterial solution increased by 0.29. Similarly, Zhang et al. [37] explored nitrate removal. They found that low voltage introduced to nitrifying bacteria (500–700 mV) effectively facilitated their proliferation and activity, efficiently removing nitrate from groundwater. Liu et al. [38] proposed the technique of weak microbial current to manage water body eutrophication. By stimulating bacteria with a weak current of 0.2 V, the remediation rate of nitrate nitrogen in the water body was substantially enhanced by boosting bacterial proliferation. These findings demonstrate that introducing an appropriate electric field to bacteria can enhance bacterial accumulation and facilitate subsequent research procedures.

3.2.2. The Influence of Applied Electric Potential on the pH and Viability of Bacterial Liquid

The alteration in pH value impacts the metabolic activity of *S. pasteurii*. The effects of pH on microorganisms primarily manifest in the following aspects: ① Affecting microbial activity, as the most favourable pH for *S. pasteurii* is approximately 9.2. Values that are too high or too low can affect its biological activity; ② modifying the permeability of the cell membrane, which influences the absorption of nutrients by microorganisms in the environment; and ③ enhancing the toxic effect of microbial metabolites on microbes, which can impede the proliferation of microbes and their utilization of nutrients.

Figure 8 illustrates the effect of electrification on the pH value of the bacterial liquid. Fluctuations in pH value are observed in the bacterial liquid under each potential gradient, compared to the control group at 0 V/cm. The best promotion of bacterial regrowth occurs under a gradient of 0.5 V/cm. Due to the high OD₆₀₀ of the bacterial solution used, there is a high consumption of nutrients in the medium, resulting in a limited pH increase under the electric potential gradient. Nonetheless, the overall trend still demonstrates the growth and inhibition of bacteria under each gradient. The change in pH value corresponds to the growth curve, with the bacterial concentration increasing under the gradient of 0.5–0.75 V/cm and the pH value rising accordingly. In the later stages, the bacterial concentration of the bacterial solution stabilizes, and the pH change decreases gradually.

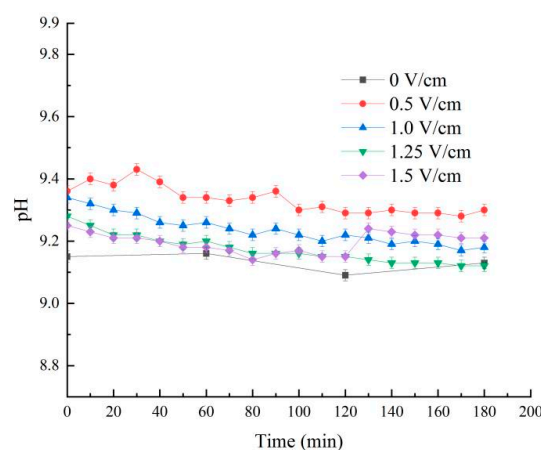


Figure 8. pH of bacterial liquid under different electric potential gradients.

In order to investigate the impact of the applied electric field on the activity of the bacterial liquid, samples were taken every thirty minutes for conductivity measurements. The urease activity was transformed using the conductivity conversion Formulas (7) and (8), and the specific changes are depicted in Figure 9. During the initial stage of electrification, the electric field caused the surface potential of the cell membrane of the bacteria to change,

which in turn affected the membrane's permeability. The difference in osmotic pressure inside and outside the bacterial cell enabled the culture environment's nutrients to enter the bacterial body more efficiently. Furthermore, anode electrolysis produced oxygen [39], promoting the proliferation and metabolism of bacteria. This phenomenon was particularly notable at lower potential gradients. At a gradient of 0.5 V/cm, the urease activity increased gradually with the concentration of the bacterial solution. However, in the later stage, the bacteria began to decay progressively due to nutrient depletion, reducing the bacterial liquid's activity. When the potential gradient was 0.75 V/cm, the bacterial concentration increased rapidly due to the promotion effect caused by the initial electric field.

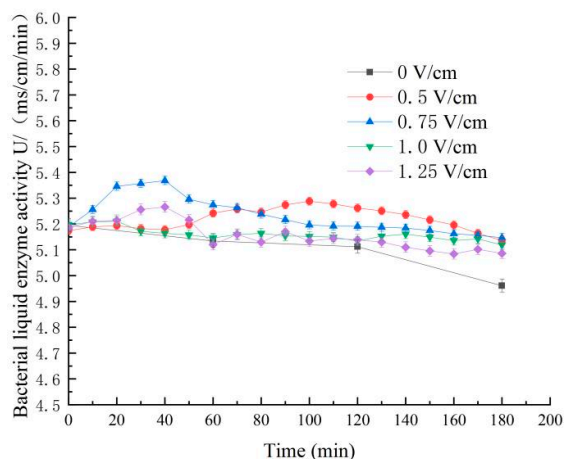


Figure 9. Changes in Enzyme Activity in Bacteria Liquid under Different Electric Potential Gradients.

Nevertheless, the continued electrification led to the rupture of the bacterial cells. The intracellular urease in the bacterial cells was released into the surrounding cultural environment, causing the bacterial cells' breakdown and mixing with the extracellular urease. The total number of urease enzymes increased during the sampling for conductivity measurement, which hastened the measured conductivity value change rate, thus enhancing the activity. Subsequently, urease activity continued to decline due to the inhibition of the electric field.

The results indicate that, according to [40], microbial growth and urease activity are better when the pH value of the microbial solution is within the range of 6.0–10.0. Notably, the microbial growth and urease activity are more favourable at a pH of 7.0–9.0 under normal culture conditions. The pH value can influence the permeability of microbial cell membranes, consequently affecting the absorption and transformation of nutrients by bacteria. Furthermore, the pH value substantially impacts the enzyme production rate and urease activity stability. The study also reveals that microbial growth and urease activity exhibit a strong positive correlation, with better microbial growth resulting in higher urease activity. The optimal pH range for the microbial solution under normal culture conditions is 7.0–9.0, with favourable microbial growth and urease activity. The pH and urease activity of the bacteria solution after the electrified culture have slightly improved compared to existing research results.

Moreover, compared with the bacteria solution under normal culture conditions by other researchers, the pH of the solution after electrification has increased by approximately 0.4. As the bacterial concentration increases, more urease is secreted. Urea is hydrolyzed by urease to form ammonia, which further hydrolyzes to form ammonium and hydroxide ions. According to Ferris et al. [41], hydroxide ions can aid in increasing the pH value surrounding cells, thereby promoting its increase. An elevated pH value can facilitate the transformation of bicarbonate ions into carbonate ions, which, under the influence of exogenous calcium ions, can encourage the formation of calcium carbonate precipitation [42]. Similarly, DeJong et al. [43] have shown that an alkaline environment is more favourable for forming calcium carbonate precipitation.

3.2.3. Effect of Applied Electric Potential on the Survivability of *S. pasteurii*

The *S. pasteurii* cells were found to have a negative charge during the experiment. Previous research suggests that the biological activity of bacteria can be activated by a weak electric field [44]. This is because the hydrogen and oxygen produced by electrolysis in a weak electric field can promote the growth of bacteria, enhance membrane permeability, and accelerate nutrient exchange in the culture environment. In order to investigate the number of viable bacteria at different electric potential gradients as the concentration changes, the bacterial solution was divided into sections every 30 min and plated. The changing trend of viable bacteria is illustrated in Figure 10. The results show that the change in viable bacteria, as measured by CFU, is highly consistent with the changing trend of OD₆₀₀. During the initial phase of electrification, the bacterial concentration substantially rose under the 0.75 V/cm gradient, leading to a corresponding rapid increase in viable bacteria. However, upon suppression of the electric field, the bacterial concentration and viable bacteria count subsequently decreased. The weak electric field generated by the 0.5 V/cm potential gradient significantly affected the growth activity and cell proliferation of *S. pasteurii*, as evidenced by the relatively stable growth trend of the number of viable bacteria. As the number of bacteria increased, the activity of the bacterial liquid also increased, and the ability of the urease produced by the bacteria to decompose urea was further strengthened, which promoted the proliferation of the pH value of the culture environment. Compared to higher potential gradients such as 1.0 V/cm and 1.25 V/cm, the number of viable bacteria was relatively unchanged due to the suppression of the electric field. A reduced magnitude of potential gradient (e.g., 0.5 V/cm) demonstrated a favorable impact on bacterial proliferation, presenting a potential avenue for further experimental investigations.

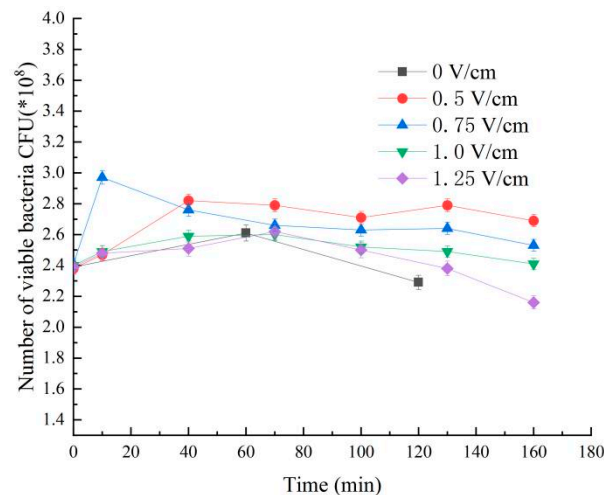


Figure 10. Changes in bacterial survival under different electric potential gradients.

4. Effect of Electric Field on the Process of Bacteria-Induced Calcium Carbonate Mineralization

4.1. The Amount of Calcium Carbonate Produced

S. pasteurii induces mineralization through calcium carbonate precipitation (MICP), which is facilitated by the urease produced by its metabolism. This enzyme hydrolyzes urea, releasing carbonate ions that combine with external calcium ions to form calcium carbonate crystals. The main reactions involved are as follows.



The concentration of the cementing liquid, alongside the proportionality of bacterial and cementing liquid (i.e., the amalgamated fluid), will play a pivotal role in precipitation induction. According to present-day research, the optimal amalgamation for forming calcium carbonate crystals and cementing efficacy transpires at a cementing liquid concentration of 1 mol/L. The mixed solution ratio is 1:4. This ratio and concentration yield the

highest utilization of effective ingredients in the cementing liquid [45], which is why they are employed in this experiment.

The steps for this method are as follows. Pour 500 mL of cultured bacterial liquid into the aseptic operation table's culture tank and place it into the hot bath. Connect the electrode and circuit and turn on the power. Start the magnetic stirrer and add 2 L of urea and calcium chloride cementing liquid through the peristaltic pump. Observe and document the precipitation reaction process. The bacterial cells play a vital role in inducing mineralization. Besides producing urease and increasing the environmental pH during growth, providing nucleation sites for forming calcium carbonate crystals is crucial. During precipitation, the calcium ions in the cementitious solution first adsorb on the bacterial cell membrane's surface. Subsequently, the area that diffuses into the bacteria generates carbonate ions under the intracellular urease's influence, which are then released outside the membrane and precipitate with calcium ions. As the residue settles, the bacteria become entirely encapsulated, and their inability to grow causes them to die.

The variation in calcium carbonate content resulting from the reaction of a mixed solution under the influence of different electric potential gradients is illustrated in Figure 11. The graph portrays a downward parabolic trend, with 84.22 g as the reference value for the calcium carbonate content when no electrical input is provided (i.e., 0 V/cm). Upon activation, the 0.5 V/cm gradient significantly enhances the efficacy of the bacterial liquid, leading to a 9.78% surge in the final calcium carbonate amount, which reaches 92.45 g. As the potential gradient becomes stronger, the effect of the electric field on the growth and precipitation of liquid bacterial changes from promoting to inhibiting. At 0.75 V/cm, the overall concentration of the bacterial solution increases, resulting in an approximate 4.37% increase in calcium carbonate precipitation compared to the scenario without electrical stimulation. The bacterial decay rate accelerates, causing a 35.80% reduction in the calcium carbonate content under a potential gradient of 1.25 V/cm. The least amount of precipitation is observed under this condition. These findings provide additional evidence that an appropriate external potential can enhance the biological activity of the bacterial liquid, the calcium carbonate precipitation is further stimulated, and the microorganism mineralization process is expedited.

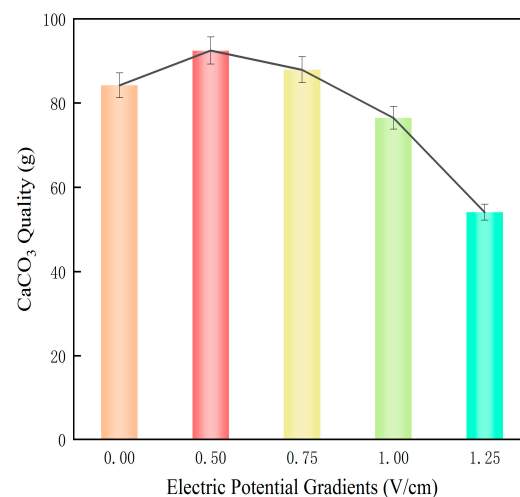


Figure 11. The Effect of Various Electric Potential Gradients on Calcium Carbonate Formation.

4.2. Changes in Crystal Form

4.2.1. Micro-Morphology and Infrared Analysis

The heterogeneous solution was filtrated and desiccated to procure a comprehensive calcium carbonate sediment, and the corresponding calcium carbonate precipitates were isolated. Naked-eye observation revealed that the sediments acquired at different electrical potentials presented different characteristics. Without electric potential, the precipitate exhibited a dense texture, tight cementation between particles, and a flat cross-sectional

area of calcium carbonate during sampling. As the electrical voltage escalated, the quantity of calcium carbonate altered, and the adhesion strength between calcium carbonate crystals, the hierarchical ordering of crystal accumulation, crystal structure, and particle size were markedly impacted.

To further investigate the influence of the applied electric field on the microbial-induced calcium carbonate cementation effect, the microscopic crystal structure of calcium carbonate precipitated in specific areas was observed and analyzed using scanning electron microscopy (SEM) and infrared spectroscopy (FT-IR). The surface microstructure of calcium carbonate under different potential gradients is depicted in Figure 12. At a constant temperature of 30 °C, the calcium carbonate deposited without electricity (Figure 12A,B) formed aggregates of various sizes, lacking a distinct morphology in appearance. However, it exhibited a tight connection between particles, dense pore filling, and an impressive cementation effect. Infrared spectroscopy analysis (Figure 12C) indicated that the crystals were a mixture of calcite and vaterite types, as demonstrated by 1421 cm^{-1} , 1082 cm^{-1} , 878 cm^{-1} , 745 cm^{-1} , and 712 cm^{-1} absorption peaks. It is worth mentioning that the peaks observed at 1421 cm^{-1} , 878 cm^{-1} , and 712 cm^{-1} corresponded to the distinctive absorption peaks of calcium carbonate with calcite structure (at V3, V2, and V4, respectively), whereas those at 1082 cm^{-1} and 745 cm^{-1} corresponded to vaterite type calcium carbonate (at V1 and V4), suggesting that the crystal structure was primarily composed of calcite. When a gradient of 0.5 V/cm was applied, the calcium carbonate precipitates assumed polygonal shapes with distinct edges and corners (Figure 12D,E), exhibiting several ellipsoid structures. The crystals were cemented together, and the pores at the junctions between the calcium carbonate crystals were expanded, reducing cementation compactness but improving the overall cementation effect. The infrared analysis revealed that the characteristic absorption peaks of calcium carbonate with calcite structure manifested at 1419 cm^{-1} and 712 cm^{-1} , whereas the distinctive peaks of vaterite-type crystals escalated. The absorption peaks at 874 cm^{-1} and 748 cm^{-1} , respectively, at V2 and V4, was mainly due to out-of-plane and in-plane bending vibrations. Finally, when the potential gradient was increased to 0.75 V/cm, the calcium carbonate precipitates began agglomerating in a small volume (Figure 12G,H). Although the crystals were closely connected, large fractured pores were observed between the blocks, and the mutual cementation effect was reduced.

Furthermore, the quantity of ellipsoidal formations within the calcium carbonate crystals exhibits an increase. Many agglomerated ellipsoidal crystals adhere to a limited number of polygonal crystal structures, leading to a division in structural hierarchy. Infrared spectrum analysis (Figure 12I) reveals that most absorption peaks lie at 1404 cm^{-1} , 1082 cm^{-1} , 874 cm^{-1} , and 742 cm^{-1} , all indicative of vaterite calcium carbonate. Compared with a 0.5 V/cm gradient and the absence of electrical influence, the characteristic calcite-type absorption peak at 1420 cm^{-1} shifts, mainly due to the anti-symmetric stretching vibration of the C-O bond under the effect of electrification, resulting in the emergence of a weak calcite-type absorption at 1439 cm^{-1} . Coupled with SEM outcomes, the calcium carbonate formed at a 0.75 V/cm gradient is chiefly of the vaterite type with a small number of calcite crystals. As the potential gradient increases, the spherical structure becomes dominant in the calcium carbonate precipitate crystals formed by the influence of a gradient ranging from 1.0 to 1.25 V/cm (illustrated in Figure 12J,K,M,N). The crystal shapes are regular and spherical, and their distribution is relatively uniform due to the crystal shapes, with no apparent edges or corners. The particles fuse and accumulate, forming a whole with significant pores and poor structural stability. Through infrared spectrum analysis (as demonstrated in Figure 12L,O), the prominent absorption peaks consist of 1401 cm^{-1} , 874 cm^{-1} , 748 cm^{-1} , 745 cm^{-1} , and so on. By consulting the infrared characteristic absorption peak data of various crystal forms, it becomes apparent that only vaterite calcium carbonate exists.

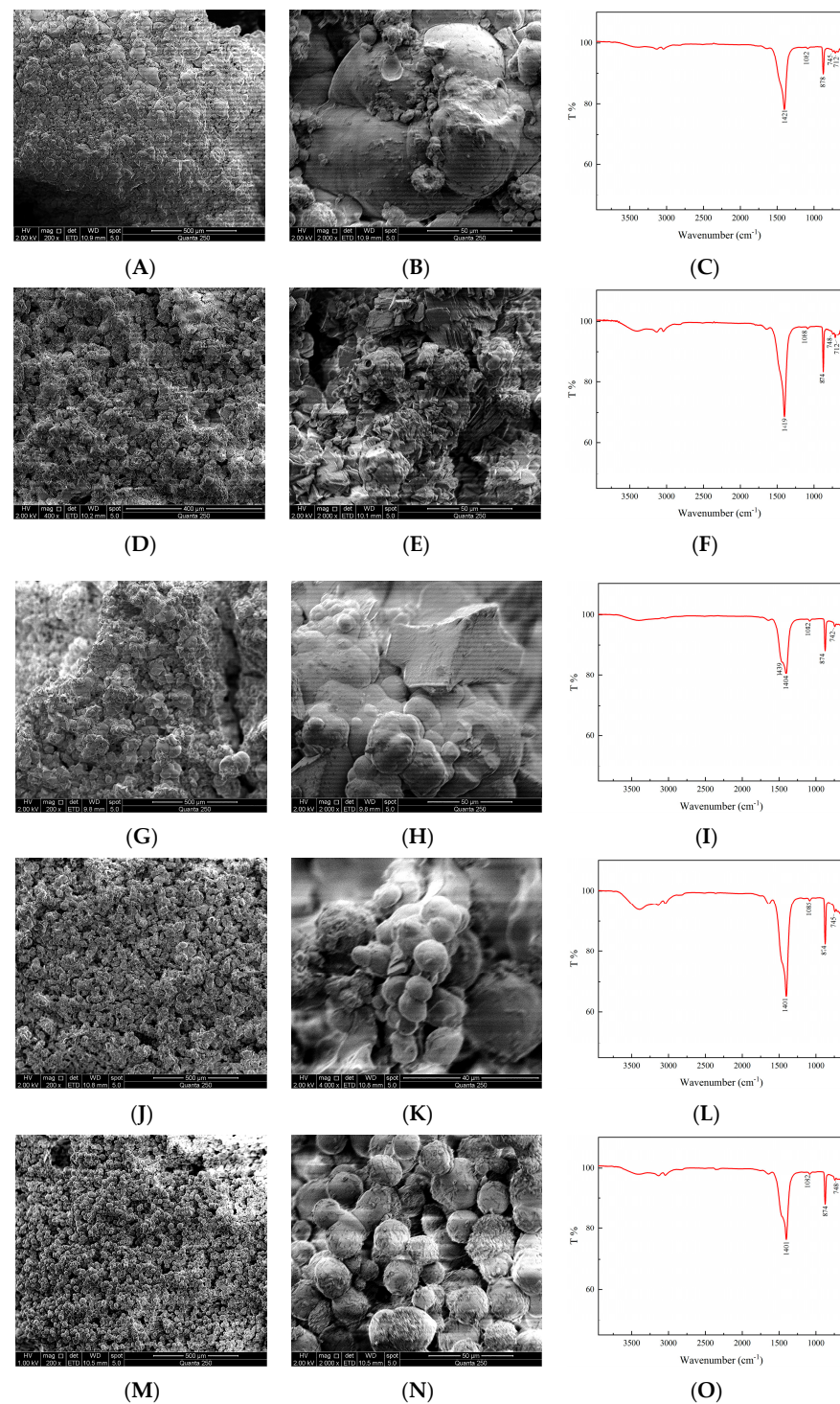


Figure 12. Effects of different potential gradients on the structure of calcium carbonate, (SEM) 0 V/cm: (A,B); 0.5 V/cm: (D,E); 0.75 V/cm: (G,H); 1.0 V/cm: (J,K); 1.25 V/cm: (M,N). (FT-IR) 0 V/cm: (C); 0.5 V/cm: (F); 0.75 V/cm: (I); 1.0 V/cm: (L); 1.25 V/cm: (O).

After comparing and analyzing the infrared spectra obtained from each group, it was discovered that the characteristic peaks of the CO_3^{2-} out-of-plane bending vibration and anti-symmetric stretching vibration underwent a redshift to 878 cm^{-1} and 1421 cm^{-1} , respectively, upon the introduction of a potential gradient and a shift to low wave velocity. The crystal morphology of calcium carbonate underwent a gradual transformation from a mixed crystal form comprising calcite and vaterite to a preponderance of vaterite crystal

form. At the same time, the crystal size of calcium carbonate also changed from irregular polycrystalline aggregates to uniform vaterite crystals with a grain size of around 20 μm . These observations suggest that the potential gradient played a significant role in inducing the formation of calcium carbonate.

Calcium carbonate manifests in various structural forms, such as calcite, vaterite, aragonite, and amorphous structures. Of all these forms, calcite boasts the highest stability and consolidation efficacy. Conversely, vaterite proves vulnerable in standard environmental settings, possessing a bad thermodynamic equilibrium. Consequently, as five groups of potential gradients impose their influence, the structural soundness of calcium carbonate produced gradually diminishes. As the potential increases, the crystal structure of calcium carbonate transmutes from stable calcite to unstable vaterite. According to research, the calcium carbonate synthesized via the MICP reaction comprises polyhedral, ellipsoidal, and a few spherical crystals with multiple edges. Such crystals will likely exhibit superior curative properties via microbial cementation [46]. Hence, in practical applications, the curing efficiency of calcium carbonate precipitated by a 0.5 V/cm gradient in this experiment should surpass that of other groups. Moreover, the content of bacteria-induced calcium carbonate is highest under this gradient.

4.2.2. Sediment Composition

In order to investigate the crystal composition of MICP reaction products in an electric field, three different calcium carbonate precipitates (0 V/cm, 0.5 V/cm, and 1.25 V/cm) underwent X-ray diffraction (XRD) analysis, building upon the results of SEM and FT-IR analyses.

The X-ray diffraction pattern depicted in Figure 13 exhibits the calcium carbonate sediment under three distinct potential gradients, with the angle denoting the abscissa and the intensity representing the ordinate. The outcome of the analysis suggests that, in the absence of electricity, the calcium carbonate precipitate crystals consist mainly of calcite, with vaterite accounting for a certain proportion. Most calcium carbonate precipitate crystals comprised calcite when introducing a potential gradient of 0.5 V/cm. As the electric potential gradient increased, the composition of calcium carbonate crystals underwent an observable change, with vaterite, dominant at 1.25 V/cm, providing additional support for the regulation of the curing reaction of microbial-induced calcium carbonate precipitation (MICP) to form calcium carbonate crystals via the introduction of an electric field. Furthermore, the XRD diffraction pattern analysis results complement the trend observed in microscopic observation results of calcium carbonate sediments, indicating a correlation between the two.

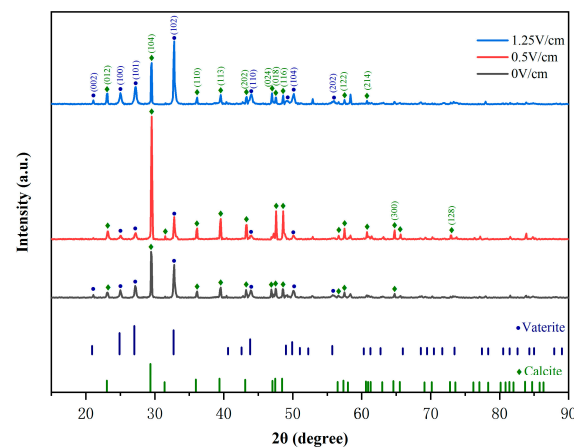


Figure 13. X-ray Diffraction Pattern of Calcium Carbonate Precipitates.

Researchers have posited that the strength growth mechanism of MICP curing is attributed to differences in the crystal structure of calcium carbonate deposits. When calcite serves as the primary material, it yields better reinforcement effects due to its ability to bond more effectively with the surface of particles when present in a higher proportion

within the calcium carbonate deposits. According to Gebauer et al. [47], calcite is a more stable polycrystalline form of calcium carbonate and may possess a higher binding strength in clusters than in other types. Zheng et al. [48] found that after using egg white to regulate the crystal form of calcium carbonate in the MICP reaction, the 5% egg white group, which had the highest calcite proportion, exhibited the highest cementing strength. Additionally, Zhang et al. [18] discovered that different concentrations of organic matter are crucial in regulating calcium carbonate's morphology and crystal structure in MICP reinforcement research when another organic matter is added. The calcite crystal form is the primary type of calcium carbonate. When mixed with a certain vaterite crystal form, it can better match and reinforce the pore structure of the sample, enhance the bite force between calcium carbonate and sample particles, and improve the reinforcement effect. Therefore, the calcium carbonate precipitate induced by the electric field has multi-structure characteristics in crystal form. The calcium carbonate induced by the 0.5 V/cm potential gradient has good integrity and a high calcite content, making it highly effective for solidification.

5. Discussion

This study explored the impact of *S. pasteurii* on calcium carbonate production induced by a potential gradient. The findings demonstrate that optimal electrification via a suitable electric potential gradient stimulates bacterial growth, urease activity, nutrient utilization, and urea hydrolysis rate. This, in turn, expedites the induced mineralization of microorganisms, thereby elevating calcium carbonate production. However, elevated potential gradients can stifle bacterial growth and urease activity, causing the induced calcium carbonate content to decline. *S. pasteurii* plays a dual role in microbial-induced calcium carbonate deposition. Firstly, the strain synthesizes urease within the cell, accelerating urea hydrolysis [49,50]. Secondly, *S. pasteurii* can serve as nucleation sites of calcium carbonate, thus promoting the formation of calcium carbonate crystals. The crystal structure of calcium carbonate influenced by microorganisms transforms a potential gradient that acts upon it. The original mixed crystal form of calcite and vaterite gradually shifts to a vaterite-dominated crystal form. The crystal particles transition from an irregular divergent distribution to uniform distribution. Additionally, the microbial mineralization process involves the growth of calcium carbonate crystals. Early stage calcium carbonate crystals facilitate the implantation and formation of the induced calcium carbonate later. Calcium carbonate deposits merge, allowing bacteria and enzymes to effectively aggregate at crystal particles' superposition, offering an additional nucleation site for biological deposition. Gradually, calcium carbonate particles coalesce and chelate into larger particle aggregates.

Although the electric field notably promotes MICP technology, further optimization is necessary to address certain limitations. In terms of energy consumption, the electric field requires a certain amount of energy, including electrodes, power supplies, and other materials, and future considerations should prioritize its economy. Operation and control of the electric field require specific management, including controlling the size and duration of the field, which should be optimized and adjusted throughout the process. Additionally, the test scale may affect the application effect due to laboratory conditions. Thus, the controllable range should be optimized according to the specific situation. Therefore, proper optimization and control of MICP technology by an electric field are essential in enhancing its application effect and economy.

Microbial mineralization is extensively used in the environmental treatment and soil reinforcement due to its ecological compatibility and economic benefits, but some challenges still need to be addressed. For instance, basic research on molecular mechanisms such as high-efficiency urease activity is relatively lacking. Furthermore, it remains unclear if microbial mineralization reactions have a special value in the physiological sense of bacteria themselves. More systematic research is necessary to induce the crystal structure and morphology of calcium carbonate crystals.

This paper explores the impact of electric potential gradient on microbial mineralization based on MICP technology. However, the research duration and experimental ratio gradient level are relatively limited. To better understand the regulation of the electric field on microbial-induced calcium carbonate crystal structure and the change in crystal content, it is necessary to strengthen the metabolic mechanism of microorganisms and promote the application effect of microbial mineralization in various fields.

6. Conclusions

In this study, we employed microbial-induced calcium carbonate precipitation (MICP) technology to enhance the growth and activity alterations of *S. pasteurii* under the most favorable culture conditions with various potential gradients to investigate the impact of the electric field on microbial-induced mineralization. The findings demonstrated the following outcomes: (1) The highest concentration of bacteria was achieved after 24 h, accompanied by the highest level of urease activity. Additionally, the specific number of viable bacteria was determined by coating the plate, and the bacteria solution corresponding to the maximum value of OD₆₀₀ was subjected to an electric charge. (2) An appropriate applied electric field can enhance the activity of *S. pasteurii*, with a notable promotion effect observed under a lower gradient. Moreover, this led to accelerated bacteria growth, improved material utilization rate and urease activity, elevated pH levels within the culture environment, optimized bacteria mineralization, and increased calcium carbonate production. However, with the increase in the potential gradient, the inhibitory effect on the bacterial liquid gradually increased. (3) Calcium carbonate sedimentation was most significant at a gradient of 0.5 V/cm, which was closely linked to the promotion effect of the electric field on the bacterial solution. Furthermore, the crystal shapes of calcium carbonate under different potential gradients were significantly different. The calcium carbonate crystal formed under a low potential gradient was composed of calcite and vaterite, which exhibited substantial cementing effects. In contrast, the calcium carbonate crystal formed under a high potential gradient was primarily vaterite, which exhibited poor thermodynamic stability. Therefore, from an application perspective, the calcium carbonate crystal with a 0.5 V/cm gradient was found to have the most optimal effect, content, and suitable crystal shapes.

7. Significance and Suggestions of Research

The microbial-induced calcium carbonate precipitation (MICP) technology exhibits promising application prospects in various engineering fields. However, there exist several scientific issues that need to be addressed before its practical implementation, such as the by-products generated during the microbial culture process [51], reinforcement uniformity [18], environmental impact [52], process cost, and others [53]. The effect of electric fields on MICP technology is of significant importance. This study introduced an electric field during the precipitation of *S. pasteurii* culture and calcium carbonate. The electric field facilitated the growth and cellular proliferation of *S. pasteurii*. It improved the bacteria's metabolism and enzyme activity, thereby increasing the yield of calcium carbonate and providing more nucleation sites for precipitation. This ultimately reduced the cost of culture materials, making them highly valuable for practical applications. Additionally, the electric field regulated the crystal structure and arrangement of the calcium carbonate induced by *S. pasteurii*, resulting in improved compactness and homogeneity of the cemented precipitation products. Furthermore, it is speculated that the subsequent application of an electric field in MICP reinforcement of porous media could enhance the deposition and mutual cementation between bacteria and calcium carbonate precipitation, thereby improving the cementation performance and shear strength of microbial support of porous media.

Introducing an electric field into MICP technology has widened its potential applications, including surface reinforcement of porous media, such as groundwater and industrial wastewater pollution control, rock and soil improvement, waterproofing, and impermeability. In order to overcome the challenges that impede the development of this technology, more research is necessary to optimize the application of MICP technology,

reduce by-product generation, develop new and improved technology, and use computer simulation analysis to enhance the reinforcement effect of MICP. Furthermore, efforts should be directed towards breeding specific urea-dissolving bacteria, stimulating in situ microorganisms to produce a cementation performance, and conducting detailed research to improve and apply MICP technology.

Author Contributions: Conceptualization, J.D. and M.L.; methodology, L.W.; software, L.H.; validation, J.D. and Z.Z.; formal analysis, L.W.; investigation, Y.T.; resources, M.L.; data curation, Y.T.; writing—original draft preparation, J.D.; writing—review and editing, J.D. and M.L.; visualization, L.H.; supervision, Z.Z.; project administration, L.W. and Z.Z.; funding acquisition, L.W. and Z.Z. All authors have read and agreed to the published version of the manuscript.

Funding: This research was funded by the National Natural Science Foundation of China (grant number: 52274167), the Natural Science Foundation of Hunan Province (grant numbers: 2022JJ40374), the Research Foundation of Education Bureau of Hunan Province (grant numbers: 22B0410, 20B496), the Hengyang City Science and Technology Program Project Funding (grant numbers: 202150063769), the Hunan Province’s technology research project “Revealing the List and Taking Command” (grant numbers: 2021SK1050).

Data Availability Statement: Not applicable.

Conflicts of Interest: The authors declare no conflict of interest.

References

1. Miller, S.A. The role of cement service-life on the efficient use of resources. *Environ. Res. Lett.* **2020**, *15*, 024004. [[CrossRef](#)]
2. Schneider, M.; Romer, M.; Tschudin, M.; Bolio, H. Sustainable Cement Production—Present and Future. *Cem. Concr. Res.* **2011**, *41*, 642–650. [[CrossRef](#)]
3. Feng, J.; Chen, B.; Sun, W.; Wang, Y. Microbial induced calcium carbonate precipitation study using *Bacillus subtilis* with application to self-healing concrete preparation and characterization. *Constr. Build. Mater.* **2021**, *280*, 122460. [[CrossRef](#)]
4. Sj, A.; Sg, B.; Msr, A. Influence of biogenic treatment in improving the durability properties of waste amended concrete: A review. *Constr. Build. Mater.* **2020**, *263*, 120170.
5. Yu, X.; Jiang, J.; Liu, J.; Li, W. Review on potential uses, cementing process, mechanism and syntheses of phosphate cementitious materials by the microbial mineralization method. *Constr. Build. Mater.* **2020**, *273*, 121113. [[CrossRef](#)]
6. Zheng, T.; Qian, C. Self-Healing of Later-Age Cracks in Cement-Based Materials by Encapsulation-Based Bacteria. *J. Mater. Civ. Eng.* **2020**, *32*, 04020341. [[CrossRef](#)]
7. Almajed, A.; Lateef, M.A.; Moghal, A.A.B.; Lemboye, K. State-of-the-art review of the applicability and challenges of microbial-induced calcite precipitation (MICP) and enzyme-induced calcite precipitation (EICP) techniques for geotechnical and geo-environmental applications. *Crystals* **2021**, *11*, 370. [[CrossRef](#)]
8. Feng, C.; Cui, B.; Ge, H.; Huang, Y.; Zhang, W.; Zhu, J. Reinforcement of recycled aggregate by Microbial-Induced mineralization and deposition of calcium carbonate—Influencing factors, mechanism and effect of reinforcement. *Crystals* **2021**, *11*, 887. [[CrossRef](#)]
9. Gao, H.; Dai, S. Influence of Culture Medium on Cementation of Coarse Grains Based on Microbially Induced Carbonate Precipitation. *Crystals* **2022**, *12*, 188. [[CrossRef](#)]
10. Lin, H.; Suleiman, M.T.; Brown, D.G. Investigation of pore-scale CaCO₃ distributions and their effects on stiffness and permeability of sands treated by microbially induced carbonate precipitation (MICP). *Soils Found.* **2020**, *60*, 944–961. [[CrossRef](#)]
11. Zhang, Z.-J.; Li, B.; Hu, L.; Zheng, H.-M.; He, G.-C.; Yu, Q.; Wu, L.-L. Experimental study on MICP technology for strengthening tail sand under a seepage field. *Geofluids* **2020**, *2020*, 8819326. [[CrossRef](#)]
12. Hoang, T.; Alleman, J.; Cetin, B.; Ikuma, K.; Choi, S.G. Sand and Silty-Sand Soil Stabilization Using Bacterial Enzyme Induced Calcite Precipitation (BEICP). *Can. Geotech. J.* **2019**, *56*, 808–822. [[CrossRef](#)]
13. Chek, A.; Crowley, R.; Ellis, T.N.; Durnin, M.; Wingender, B. Evaluation of Factors Affecting Erodibility Improvement for MICP-Treated Beach Sand. *J. Geotech. Geoenviron. Eng.* **2021**, *147*, 4021001. [[CrossRef](#)]
14. Chuo, S.C.; Mohamed, S.F.; Setapar, S.; Ahmad, A.; Ibrahim, M. Insights into the Current Trends in the Utilization of Bacteria for Microbially Induced Calcium Carbonate Precipitation. *Materials* **2020**, *13*, 4993. [[CrossRef](#)]
15. Lai, Y.; Yu, J.; Liu, S.; Liu, J.; Dong, B. Experimental study to improve the mechanical properties of iron tailings sand by using MICP at low pH. *Constr. Build. Mater.* **2020**, *273*, 121729. [[CrossRef](#)]
16. Liu, B.; Zhu, C.; Tang, C.S.; Xie, Y.H.; Shi, B. Bio-remediation of desiccation cracking in clayey soils through microbially induced calcite precipitation (MICP). *Eng. Geol.* **2019**, *264*, 105389. [[CrossRef](#)]
17. Xu, X.; Guo, H.; Cheng, X.; Li, M. The promotion of magnesium ions on aragonite precipitation in MICP process. *Constr. Build. Mater.* **2020**, *263*, 120057. [[CrossRef](#)]

18. Zhang, Z.J.; Tong, K.W.; Hu, L.; Yu, Q.; Wu, L.L. Experimental study on solidification of tailings by MICP under the regulation of organic matrix. *Constr. Build. Mater.* **2020**, *265*, 120303. [[CrossRef](#)]
19. Okwadha, G.D.O.; Li, J. Optimum conditions for microbial carbonate precipitation. *Chemosphere* **2010**, *81*, 1143–1148. [[CrossRef](#)]
20. Yu, T.; Souli, H.; Péchaud, Y.; Fleureau, J.M. Optimizing protocols for microbial induced calcite precipitation (MICP) for soil improvement—A review. *Eur. J. Environ. Civ. Eng.* **2022**, *26*, 2218–2233. [[CrossRef](#)]
21. Kitamura, M.; Konno, H.; Yasui, A.; Masuoka, H. Controlling factors and mechanism of reactive crystallization of calcium carbonate polymorphs from calcium hydroxide suspensions. *J. Cryst. Growth* **2002**, *236*, 323–332. [[CrossRef](#)]
22. Wei, S.P.; Cui, H.P.; Jiang, Z.L.; Liu, H.; He, H.; Fang, N.Q. Biomineralization processes of calcite induced by bacteria isolated from marine sediments. *Braz. J. Microbiol.* **2015**, *46*, 455–464. [[CrossRef](#)] [[PubMed](#)]
23. Xu, W.; Zheng, J.; Chu, J.; Zhang, R.; Cui, M.; Lai, H.; Zeng, C. New method for using N-(N-butyl)-thiophosphoric triamide to improve the effect of microbial induced carbonate precipitation. *Constr. Build. Mater.* **2021**, *313*, 125490. [[CrossRef](#)]
24. Nemati, M.; Greene, E.A.; Voordouw, G. Permeability profile modification using bacterially formed calcium carbonate: Comparison with enzymic option. *Process Biochem.* **2005**, *40*, 925–933. [[CrossRef](#)]
25. Gidudu, B.; Chirwa, E.M.N. The combined application of a high voltage, low electrode spacing, and biosurfactants enhances the bio-electrokinetic remediation of petroleum contaminated soil. *J. Clean. Prod.* **2020**, *276*, 122745. [[CrossRef](#)]
26. Ossai, I.C.; Ahmed, A.; Hassan, A.; Hamid, F.S. Remediation of soil and water contaminated with petroleum hydrocarbon: A review. *Environ. Technol. Innov.* **2019**, *17*, 100526. [[CrossRef](#)]
27. Mena, E.; Villasenor, J.; Canizares, P.; Rodrigo, M.A. Effect of a direct electric current on the activity of a hydrocarbon-degrading microorganism culture used as the flushing liquid in soil remediation processes. *Sep. Purif. Technol.* **2014**, *124*, 217–223. [[CrossRef](#)]
28. Cheng, F.L.; Guo, S.H.; Wang, S.; Guo, P.H.; Lu, W.J. Transportation and augmentation of the deposited soil bacteria in the electrokinetic process: Interactions between soil particles and bacteria. *Geoderma* **2021**, *404*, 115260. [[CrossRef](#)]
29. Martin, D.; Dodds, K.; Ngwenya, B.T.; Butler, I.B.; Elphick, S.C. Inhibition of *Sporosarcina pasteurii* under Anoxic Conditions: Implications for Subsurface Carbonate Precipitation and Remediation via Ureolysis. *Environ. Sci. Technol.* **2012**, *46*, 8351–8355. [[CrossRef](#)]
30. Kang, B.; Zha, F.; Li, H.; Xu, L.; Sun, X.; Lu, Z. Bio-Mediated Method for Immobilizing Copper Tailings Sand Contaminated with Multiple Heavy Metals. *Crystals* **2022**, *12*, 522. [[CrossRef](#)]
31. Ramachandran, S.K.; Ramakrishnan, V.; Bang, S.S. Remediation of Concrete Using Microorganisms. *ACI Mater. J.* **2001**, *98*, 3–9.
32. Zhao, Q.; Li, L.; Li, C.; Li, M.; Amini, F.; Zhang, H. Factors affecting improvement of engineering properties of MICP-treated soil catalyzed by bacteria and urease. *J. Mater. Civ. Eng.* **2014**, *26*, 04014094. [[CrossRef](#)]
33. Cuzman, O.A.; Richter, K.; Wittig, L.; Tiano, P. Alternative nutrient sources for biotechnological use of *Sporosarcina pasteurii*. *World J. Microbiol. Biotechnol.* **2015**, *31*, 897–906. [[CrossRef](#)] [[PubMed](#)]
34. Di, P.; Zhi-Ming, L.; Bi-Ru, H.; Wen-Jian, W. Progress on mineralization mechanism and application research of *Sporosarcina pasteurii*. *Prog. Biochem. Biophys.* **2020**, *47*, 467–482.
35. Whiffin, V.S.; Van Paassen, L.; Harkes, M.P. Microbial Carbonate Precipitation as a Soil Improvement Technique. *Geomicrobiol. J.* **2007**, *24*, 417–423. [[CrossRef](#)]
36. Sun, X.-T.; Ma, J.; Sun, X.-Y.; Liu, B. Electrolytic Stimulation of *Escherichia coli* by a Direct Current. *Microbiol./Weishengwuxue Tongbao* **2010**, *37*, 1440–1446.
37. Zhang, B.; Liu, Y.; Tong, S.; Zheng, M.; Zhao, Y.; Tian, C.; Liu, H.; Feng, C. Enhancement of bacterial denitrification for nitrate removal in groundwater with electrical stimulation from microbial fuel cells. *J. Power Sources* **2014**, *268*, 423–429. [[CrossRef](#)]
38. Liu, H.; Ouyang, F.; Chen, Z.; Chen, Z.; Lichtfouse, E. Weak electricity stimulates biological nitrate removal of wastewater: Hypothesis and first evidences. *Sci. Total Environ.* **2021**, *757*, 143764. [[CrossRef](#)]
39. Rabbi, M.F.; Clark, B.; Gale, R.J. In situ TCE bioremediation study using electrokinetic cometabolite injection. *Waste Manag.* **2000**, *20*, 279–286. [[CrossRef](#)]
40. Yi, H.; Zheng, T.; Jia, Z.; Su, T.; Wang, C. Study on the influencing factors and mechanism of calcium carbonate precipitation induced by urease bacteria. *J. Cryst. Growth* **2021**, *564*, 126113. [[CrossRef](#)]
41. Ferris, F.G.; Phoenix, V.; Fujita, Y.; Smith, R. Kinetics of calcite precipitation induced by ureolytic bacteria at 10 to 20 C in artificial groundwater. *Geochim. Cosmochim. Acta* **2004**, *68*, 1701–1710. [[CrossRef](#)]
42. Ng, W.-S.; Lee, M.-L.; Hii, S.-L. An overview of the factors affecting microbial-induced calcite precipitation and its potential application in soil improvement. *Int. J. Civ. Environ. Eng.* **2012**, *6*, 188–194.
43. DeJong, J.T.; Mortensen, B.M.; Martinez, B.C.; Nelson, D.C. Bio-mediated soil improvement. *Ecol. Eng.* **2010**, *36*, 197–210. [[CrossRef](#)]
44. Wick, L.Y.; Shi, L.; Harms, H. Electro-bioremediation of hydrophobic organic soil-contaminants: A review of fundamental interactions. *Electrochim. Acta* **2007**, *52*, 3441–3448. [[CrossRef](#)]
45. Cheng, L.; Qian, C.; Wang, R.; Wang, J. Study on the mechanism of calcium carbonate formation induced by carbonate-mineralization microbe. *Acta Chim. Sin.* **2007**, *65*, 2133–2138.
46. Rong, H.; Qian, C.-X.; Li, L.-Z. Study on microstructure and properties of sandstone cemented by microbe cement. *Constr. Build. Mater.* **2012**, *36*, 687–694. [[CrossRef](#)]
47. Gebauer, D.; Volkel, A.; Colfen, H. Stable prenucleation calcium carbonate clusters. *Science* **2008**, *322*, 1819–1822. [[CrossRef](#)]

48. Zheng, H.-M.; Wu, L.-L.; Tong, K.-W.; Ding, D.-X.; Zhang, Z.-J.; Yu, Q.; He, G.-C. Experiment on microbial grouting reinforcement of tailings under the regulation of egg white. *Soils Found.* **2020**, *60*, 962–977. [[CrossRef](#)]
49. Muynck, W.D.; Belie, N.D.; Verstraete, W. Microbial carbonate precipitation in construction materials: A review. *Ecol. Eng.* **2010**, *36*, 118–136. [[CrossRef](#)]
50. Stocks-Fischer, S.; Galinat, J.K.; Bang, S.S. Microbiological precipitation of CaCO₃. *Soil Biol. Biochem.* **1999**, *31*, 1563–1571. [[CrossRef](#)]
51. Naveed, M.; Duan, J.; Uddin, S.; Suleman, M.; Hui, Y.; Li, H. Application of microbially induced calcium carbonate precipitation with urea hydrolysis to improve the mechanical properties of soil. *Ecol. Eng.* **2020**, *153*, 105885. [[CrossRef](#)]
52. Li, M.; Cheng, X.; Guo, H. Heavy metal removal by biomineralization of urease producing bacteria isolated from soil. *Int. Biodeterior. Biodegrad.* **2013**, *76*, 81–85. [[CrossRef](#)]
53. Rahman, M.M.; Hora, R.N.; Ahenkorah, I.; Beecham, S.; Karim, M.R.; Iqbal, A. State-of-the-art review of microbial-induced calcite precipitation and its sustainability in engineering applications. *Sustainability* **2020**, *12*, 6281. [[CrossRef](#)]

Disclaimer/Publisher’s Note: The statements, opinions and data contained in all publications are solely those of the individual author(s) and contributor(s) and not of MDPI and/or the editor(s). MDPI and/or the editor(s) disclaim responsibility for any injury to people or property resulting from any ideas, methods, instructions or products referred to in the content.